STUDY ON THE SURFACE CHANGES OF HEAT-TREATED ASPEN WOOD DUE TO AGING BY DIFFERENT TECHNIQUES

Kocaefe D.*, Huang X., Kocaefe Y.
*Author for correspondence
Department of Applied Sciences
University of Québec at Chicoutimi
555, boul. de l'Université, Chicoutimi, Québec, Canada,
E-mail: Duygu_Kocaefe@uqac.ca

Abstract

Heat-treated wood undergoes degradation induced by weathering factors such as solar radiation, temperature variations, rain, and snow. The aging of heat-treated wood affects significantly its surface properties. In this study, the artificial aging test of heat-treated wood using a UV chamber was carried to see the effect of aging on the wood surface. The net radiative heat transfer to the wood sample surfaces in this chamber was estimated in order to determine the corresponding natural weathering times. A complete understanding of the surface changes during the weathering process would allow the development of new treatments and finishes that would greatly enhance the durability of heat-treated wood against degradation due to weathering. Study of the heat-treated wood surface before and after weathering by different techniques helps provide an insight into the degradation process. The techniques and tools for studying heat-treated wood surfaces include color measurement, contact angle test for wettability analysis, light microscopy, FTIR, XPS, and SEM. Each technique gives information on different aspects such as chemistry, structure, and appearance. In this article, the utilization of these techniques is discussed. A number of results for different cases are presented. The aging affects the color of the tangential and radial surfaces differently. During aging, lignin decreases and OH increases; and this increases the wettability of wood.

INTRODUCTION

Heat-treatment of wood is a technique for preserving and protecting wood and involves heating wood to temperatures in the range of 180 to 240°C. Heat and mass transfer occurs during the heat-treatment process between the heating medium (usually gas) and wood, which modifies wood both chemically and physically. The process parameters during the heat treatment determine the final product quality. This treatment preserves wood without using any additional chemicals. Consequently, the wood product acquires new and attractive properties such as lower hygroscopy, higher dimensional stability, better resistance to degradation by fungus, and darker color compared to the untreated wood. These new properties add value to the product and make its use possible for indoor and outdoor applications.

In the case of outdoor applications, similar to untreated wood, heat-treated wood undergoes degradation triggered by weathering factors. Sunlight is an important cause of damage to wood materials. Ultraviolet light has long been recognized as the factor responsible for most of this damage. Accelerated weathering tests are widely used for research and development, quality control, and material certification. There is a variety of light sources to simulate sunlight in order to investigate the damage it caused to wood. Comparative spectroradiometric measurements suggest that the exposure of wood to xenon arc lamps corresponds best to the natural atmospheric exposure [1]. A number of publications on the general features of the artificial weathering of heat-treated wood are available mostly for jack pine [1-6]. However, no information is available on the calculation of natural aging time from artificial aging data on heat-treated wood. This article presents the results for the heat treatment of aspen and the determination of natural aging time.

In this study, the artificial weathering tests of heat-treated wood samples were carried out under xenon arc lamps, and their surface properties were characterized using different techniques.

MATERIALS AND METHODS

1) Materials

The aspen, *Populus tremuloides*, which is a North American species, was studied. Kiln-dried wood boards of approximately 6500 × 200 × 30 mm with a moisture content of about 12% were heat-treated up to 210°C with a heating rate of 15°C/h and a soaking time of 1h at this temperature in a prototype furnace in the wood thermotransformation laboratory of the University of Quebec at Chicoutimi (UQAC), Quebec, Canada. Hot combustion gases were used to treat the wood, and water was injected into the hot gas in order to have a certain humidity. Specimens of 30 × 30 mm cross-section on longitudinal tangential smooth surfaces and 20-mm thickness were prepared from sapwood of heat-treated and untreated wood. All samples were arbitrarily selected and stored in an environmentally controlled chamber at a temperature of 20°C and a relative humidity (RH) of 40% until they were exposed to the artificial weathering, and the characterization tests for samples aged over different periods of time were carried out as described below.

2) Artificial weathering tests

Artificial weathering tests were conducted using a Q-sun xenon test chamber (model Xe-1-B/S) as shown schematically in Figure 1. A controlled irradiance water-cooled xenon arc lamp with a daylight filter was used as the source of radiation to simulate the sunlight. Tests were performed according to ASTM G155 standard with continuous xenon light exposure without dark cycle. In this standard, the air temperature is not controlled and the air humidity is kept constant. The most common irradiance settings are 0.35 or 0.55 W/m^2 of radiant

heat flux at 340 nm wavelength. A report from the Q-sun company suggests that 0.35 W/m^2 represents winter sunlight while 0.55 W/m^2 corresponds to summer sunlight [7]. In this study, the irradiance level was set to 0.35 W/m^2 at 340 nm wavelength to better represent the conditions in Quebec. The black panel temperature was set to 63±3˚C. The irradiation was interrupted after different periods of exposure, and two samples were taken out from each set for the evaluation of their properties.

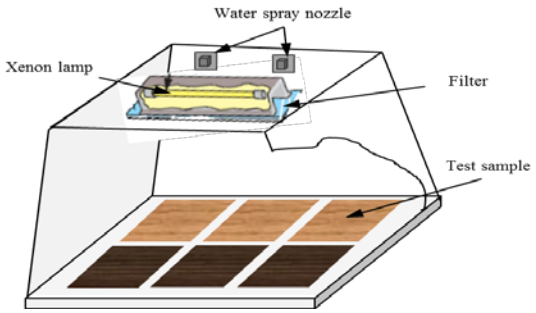

Figure 1 A schematic view of the Q-sun xenon test chamber

3) Color determination

The surface color of specimens exposed to artificial weathering for different periods was measured using a reflectance spectrophotometer (Datacolor, CHECK TM). The calibration was carried out with standards provided by the supplier. The color system L*a*b* 1976 according to the CIELab standard [8] was used to determinate the color of sample surface. The system is characterized by three parameters, L*, a*, and b* co-ordinates that represent the lightness and the color pairs red/green and yellow/ blue, respectively. The total color difference (ΔE) was calculated according to Equation (1). ΔE is a function of the artificial sunlight exposure time t.

$$\Delta E = \left[(L_t^* - L_0^*)^2 + (a_t^* - a_0^*)^2 + (b_t^* - b_0^*)^2\right]^{\frac{1}{2}} \quad (1)$$

where the subscript "0" represents the values before weathering, and "t" denotes the ones after weathering.

4) Light microscopy image analysis

Cross sections cut transversely through wood at a thickness of 7-20 μm were examined and photographed with Nikon eclipse E600 Microscope. Some sections were also stained with 0.05% aqueous toluidine blue prior to the examination with the photomicroscope. The light microscopy was also used on sections that had been stained with 1% aqueous osmium tetroxide (OsO4) for 10-30 min at room temperature. Different magnifications were used. Sections for the scanning electron microscopy (SEM) were cut from the same blocks that had been used to produce sections for light microscopy.

5) SEM analysis

Small wood blocks measuring 20 ×20 mm on the weathered tangential surface of the samples were cut from heat-treated and untreated boards after artificial sunlight irradiation for different periods of time. All blocks were sputter-coated with a palladium/gold layer for 140 s and then mounted onto standard aluminum stubs using electrically conducting paste. The samples were scanned using Jeol scanning electron microscope (JSM 6480LV). The distance between the sample and electron microscope head was 20-25 mm with a spot size of 35-50.

6) Contact angle tests

The contact angles between water and specimen surfaces were measured using a sessile-drop system (First Ten Angstroms FTA200, equipped with a CCD camera and an image analysis software). A drop of test liquid with a volume of 15μl was dosed automatically by an auto-syringe and dropped on the wood specimen placed on a movable sample table. Measurements of contact angle were carried out by the sessile-drop profile method with a view across the grain. The wettability of the wood surface by water parallel to the grain was investigated. Six to twelve tests were performed for each exposure time. The dynamic contact angle data were collected and used to assess the wood surface wettability.

7) FTIR spectroscopy analysis

The air-dried specimens were studied using Jasco FT/IR 4200 equipped with a diamond micro-ATR crystal. IR spectra were recorded in the wavenumber range of 550–4000 cm^{-1} with a 4 cm^{-1} resolution for 20 scans prior to the Fourier transformation. The incident angle of the micro-ATR crystal was 47˚ corresponding to a sampling depth of infrared radiation of 0.2–5 μm, depending on the wavenumber. The IR spectra for each set corresponding to different experimental conditions were transformed into the absorbance spectra using the Jasco spectra manager software and analyzed. The IR spectra were corrected by the FTIR software package, which includes an ATR correction algorithm. All relative intensity ratios were normalized relative to the peak of the band at 2900 cm^{-1}, which corresponds to C-H stretching in methyl and methylene groups.

8) XPS spectroscopy analysis

Small wood chips (approximately 10×10 mm of exposed surface and 1mm thickness) were cut with a cutter blade from heat-treated and untreated aspen surfaces before and after artificial weathering. The XPS measurements were performed using the AXIS Ultra XPS spectrometer (Kratos Analytical) at the Alberta Centre for Surface Engineering and Science (ACSES) of the University of Alberta. The analyses were carried out according to the procedure described in a previous publication [6].

RESULTS AND DISCUSSION

1) Estimation of total irradiation during artificial aging tests

The sun can be considered approximately a black body radiating at 5800 K. Due to the distance from the sun, the irradiation reduces to about 1373 W/m^2 outside the earth's atmosphere. Attenuation in the atmosphere (depending on the climatic conditions) results in a decrease in the irradiation reaching an object on earth's surface. This also varies with the position and the orientation of that object on earth with respect to the sun.

The fraction of the total blackbody emission, f, in a spectral band is a function of λT. The fraction for the 300-800 nm band is given below [9]:

$$\lambda_1 = 0.3\mu m, T = 5800K : \lambda_1 T = 1740\mu m \cdot K,\ f_{(0\to\lambda 1)} = 0.035$$
$$\lambda_2 = 0.8\mu m, T = 5800K :\ \lambda_2 T = 4640\mu m \cdot K,\ f_{(0\to\lambda 2)} = 0.59 \quad (2)$$
$$f_{(\lambda 1\to\lambda 2)} = 0.555$$

The measured irradiance between 300 and 800 nm of the xenon lamp used is 590.8 W/m^2 [10]. Since the shapes of E_λ vs. λ are similar for both the solar irradiation and the xenon lamp with the filter, the same fraction can be assumed to hold for the lamp-filter system. Hence, the total irradiation from this lamp can be estimated as:

$$q''_{B,rad,estimated} = \frac{590.8}{0.555} = 1075 W/m^2 \quad (3)$$

2) Determination of natural weathering time from artificial weathering time tests

Natural weathering is a long process. It can be accelerated using artificial weathering in test chambers where the samples are subjected to continuous irradiation. Even though it is difficult to simulate the natural weather conditions exactly, the artificial weathering tests can provide a basis for comparison for the aging of different materials. The artificial weathering tests in this study were carried out for a period of 1512 hours. Depending on the position of a surface on earth and climatic conditions, this will correspond to different periods of time under natural conditions. The following example is for Florida, USA, where the average yearly irradiance is 186 W/m^2 [11].

Assuming that wood has a surface emissivity of ε_B= 0.90, a solar absorptivity of α_s=0.90, and an average temperature of T_s=15°C, and the average effective sky temperature is T_{sky}=-10°C, the net radiative heat flux on the surface q'' (W/m^2) can be estimated as follows (see Figure 2).

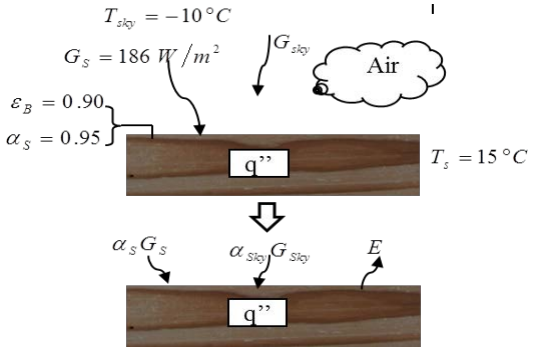

Figure 2 A schematic representation of solar irradiation on a horizontal wood surface

Under steady-state conditions, the energy balance for diffuse radiation on a horizontal surface can be written as:

$$Energy_{in} - Energy_{out} = 0 \quad (4)$$

or, per unit surface area:

$$\alpha_S G_S + \alpha_{sky} G_{sky} - E - q'' = 0 \quad (5)$$

where,

$$G_{sky} = \sigma T_{sky}^4 \quad \text{and} \quad E = \varepsilon_B \sigma T_s^4 \quad (6)$$

Since the difference between the sky temperature and the surface temperature is not too high, it can be assumed that the sky radiation is approximately concentrated in the same spectral region as that of the surface emission; then, it is reasonable to assume that:

$$\alpha_{sky} \approx \varepsilon_B = 0.90$$

Then,

$$q'' = \alpha_S G_S + \alpha_{sky} G_{sky} - E \quad (7)$$

$$q'' = \alpha_S G_S + \varepsilon_B \sigma (T_{sky}^4 - T_S^4) \quad (8)$$

Inserting the numerical values,

$$q'' = 0.90 \times 186 W/m^2 + 0.90 \times 5.67 \times 10^{-8} W/m^2 \cdot K^4 (263^4 - 288^4) K^4 \quad (9)$$

the average net heat flux on a wood surface is obtained as:

$$q'' = 167.4 W/m^2 - 106.9 W/m^2 = 60.5 W/m^2 \quad (10)$$

The relation between the artificial weathering tests and the natural weathering is as follows:

$$t_{nat} = t_{art} \times \frac{q''_{rad}}{q''} \quad (11)$$

where t_{art} is the period of time for artificial weathering, t_{nat} is the period of time for natural weathering.

For the sample that was tested in the UV chamber for 1512 h, the corresponding time for natural weathering in Florida will be:

$$t_{nat} = t_{art} \times \frac{q''_{rad}}{q''} h = 1512h \times \frac{1075 W/m^2}{60.5 W/m^2} / 24 / 365 = 3 years\ 24 days \quad (12)$$

This is the average value for a horizontal surface. Depending on the orientation of the surface (its position with respect to the direction of sunlight), this period could be somewhat longer since the horizontal surface receives the maximum irradiation. The same analysis for Canada where the average irradiation is 133 W/m^2 (for an average wood surface temperature T_s= 0°C and the average effective sky temperature T_{sky}= -25°C) gives 6 years and 4 months. Therefore, all the results in this paper correspond to around 6 years of aging in Canada.

3) Color modification of heat-treated wood during artificial weathering

Physical and chemical properties of wood are known to be a function of direction. A study of the color change on tangential (LT) and radial surfaces (LR) of the heat-treated wood was conducted to study the effect of direction on the color change during weathering (see Figure 3). The color changes more on tangential surfaces of heat-treated aspen than on radial surfaces at all weathering times. A statistical analysis (T-test) is used for the ΔE data obtained in this study. A significant difference ($P<0.05$) in the ΔE data between the two directional surfaces was found after 336 h of weathering for heat-treated aspen. This is most likely linked to the presence of different structures on different directional surfaces. During weathering, the presence of radial rays allows rapid water movement deeper into the wood structure on tangential surfaces, which is not the case for radial surfaces. Consequently, leaching with water leads to more degradation on tangential surfaces compared to radial ones.

4) Microscopic structural changes of heat-treated wood during artificial weathering

The transversal surfaces exposed to the artificial weathering test were examined with a light microscope since they are affected more by weathering. Figures 4 (a-d) present the microscopy images of heat-treated aspen before weathering (0 h) and after weathering for different exposure times. The

damage of one cell layer is visible in light microscopy image on sample surface after 72 h exposure (Figure 4 (b)). The degradation of cells and the thickness of the damaged layer increase with increasing weathering times (see Figure 4 (a-d)). Due to this damage, the separation of the damaged cells from the neighboring cells takes place after 672 h of exposure (Figure 4 (c)). Delamination and thinning of cells are present at 1512 h of exposure (Figure 4 (d)). Similar to heat-treated aspen, the first damage of untreated aspen cells that appear on the tested surface is visible at 72 h weathering (images are not presented here).

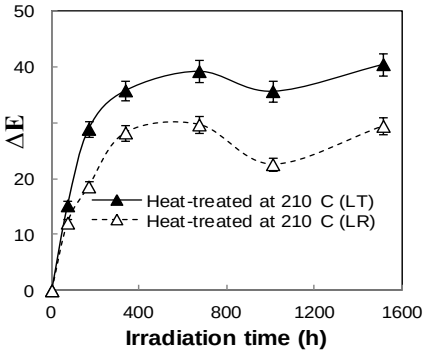

Figure 3 Comparison of color differences between tangential (LT) and radial (LR) surfaces of heat-treated wood during artificial weathering

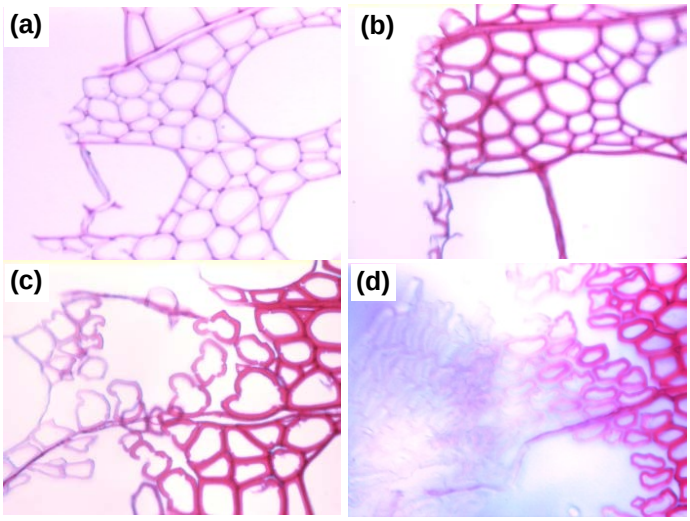

Figure 4 Light microscopy images (x50) on transverse surfaces of heat-treated aspen before and after artificial weathering for different exposure times: (a) 0 h; (b) 72 h; (c) 672 h; (d) 1512 h

Additional information on structural changes can be seen from SEM micrographs of specimen surfaces. Figures 5 (a) and (b) show the micrographs on the transverse surface of heat-treated aspen before (0 h) and after (1512 h) artificial weathering. The presence of small cracks on middle lamella, slight thinning cell wall width as well as plasticization takes place after the heat treatment of aspen. The thinning of cell wall width for the specimens can also be observed (Figure 5 (b).

Figures 5 (c) and (d) show the SEM micrographs on the longitudinal tangential surface of heat-treated specimens before (0 h) and after (1512 h) artificial weathering. SEM analysis indicates that the anatomical structure of wood is only slightly affected by heat treatment in this direction. Fibers and rays are still obvious after heat treatment. The structures of aspen (vessel elements, fibers, and axial parenchyma cells in different patterns) are present in abundance. The radial system of aspen is composed of ray parenchyma cells. The vessels appear as large cracks after weathering.

Comparison of SEM pictures in Figures 5(e) and (f) shows that while there are transverse cracks of pits, no longitudinal cracks across pits are observed on any of the pits after weathering. Pit structures on aspen surface coalesce, resulting in big transverse and ruptured cracks, followed by the formation of deep crevasses (arrow in Figure 5 (f)).

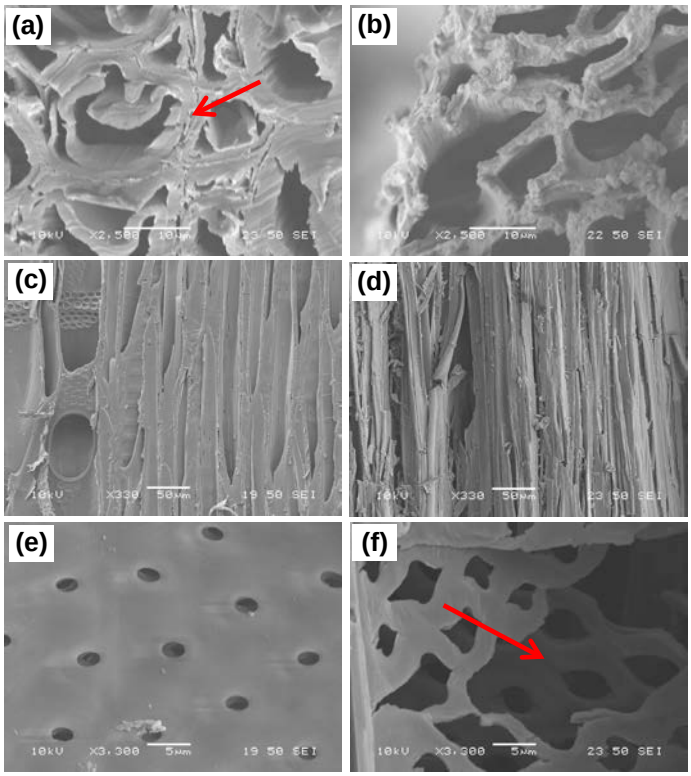

Figure 5 SEM images on transverse surfaces (a-b) and longitudinal surfaces (c-f) of heat-treated aspen before (a, c, e) and after (b, d, f) artificial weathering for 1512 h

5) Changes in wettability of wood by water during artificial weathering

Figure 6 presents the dynamic contact angles of water as a function of exposure time for heat-treated aspen on tangential surfaces. In this figure, the contact angle evolution with time is given before (0 h) and after different exposure times of weathering for specimens. As can be seen from the figure, the weathering reduces the hydrophobic behavior of the heat-treated wood; consequently, all the contact angles of weathered heat-treated wood are lower than those of unweathered wood of the same species (0 h). This shows that the artificial weathering increases the wettability of wood by water. The contact angles of heat-treated aspen decrease significantly after weathering of 72 h and continue to decrease with increasing weathering time.

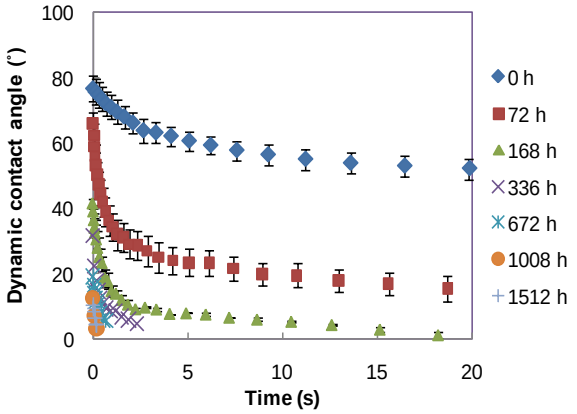

Figure 6 Dynamic contact angles of heat-treated aspen after artificial weathering for different exposure times

6) Chemical modification of heat-treated wood surfaces

To evaluate the chemical structures of the surface of heat-treated wood, high-resolution XPS spectra of C1s and O1s levels were analyzed. Other elements have very low concentrations on the surface of heat-treated and untreated wood samples of this study, which is in agreement with the results of Shen et al. [12]. All of the C1s spectra were found to consist of components related to carbon-containing functional groups. The high-resolution spectra of C1s were fitted with their decomposition into four components according to the literature [12-16]. The fitted peaks are shown in Figure 7 after curve fitting. The four peaks in deconvoluted high resolution XPS spectrum of the C1s peaks are expressed as C_1 to C_4, and these carbon bands correspond to C-C and/or C-H (C_1), C-O (C_2), C=O or/and O-C-O (C_3), and O=C-O (C_4), respectively. The high-resolution XPS spectra of C1s for heat-treated aspen samples before and after artificial weathering for 1512 h are shown in Figure 7. A careful analysis of line shape and intensity for each component on weathered surfaces shows that the XPS patterns changed considerably due to weathering. The contributions of C_1 and C_2 peaks are more important than C_3 and C_4 peaks for samples before weathering, indicating that they have higher concentrations on heat-treated sample surfaces before weathering. These two peaks are modified by the weathering process. The detailed analysis of the C1s region showed that the most important contributions for surfaces before weathering come from the C_1 class (see Figure 7 (a)), while the most important contributions for weathered surfaces come from the C_2 class (see Figure 7 (b)). C_1 peak corresponds to carbon linked to carbon (C–C) groups present in lignin, hemicelluloses, and extractives such as fatty acids and hydrogen (C-H) groups of lignin and extractives, and C_2 peak corresponds to OCH groups of lignin and C–O–C linkages of extractives and polysaccharides of wood [16]. It is important to investigate the changes of C_1 and C_2 contributions during weathering for samples heat-treated at different temperatures to study the effect of treatment temperature on the chemical elemental composition of heat-treated wood surface.

Figure 8 shows the FTIR spectra of heat-treated aspen during artificial weathering. The overall IR spectrum indicate that a number of spectral features appear to be sensitive to weathering. All the bands at 1600 cm^{-1}, 1510 cm^{-1}, 1465 cm^{-1}, 1263 cm^{-1}, and 1103 cm^{-1} represent lignin characteristics. As shown in Figure 8, all the characteristic bands of lignin decrease significantly as a result of the weathering process. This indicates that lignin is the component of heat-treated wood which is most degraded during weathering.

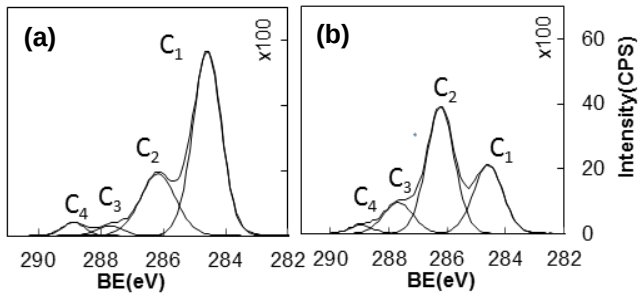

Figure 7 C1s spectra of heat-treated aspen before and after weathering for 1512 h: (a) before weathering, (b) after weathering for 1512 h

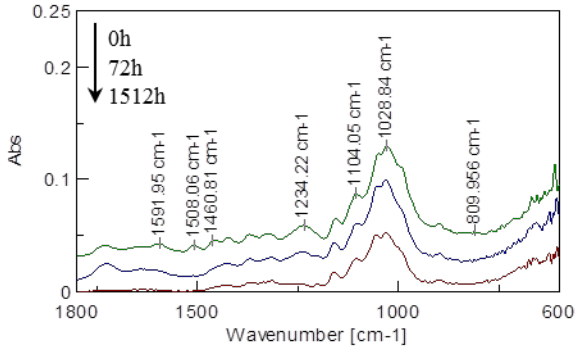

Figure 8 FTIR spectra of heat-treated aspen during artificial weathering for different exposure times

Out of the five bands mentioned above, the evolution of lignin loss is best explained by the peak at 1510 cm^{-1} of wood samples [17]. Figure 9 shows the lignin loss for heat-treated aspen after artificial weathering for different exposure times. Before weathering, heat-treated aspen surfaces have higher lignin content than untreated aspen surfaces. The results indicate that lignin is degraded gradually with increasing exposure time during artificial weathering. It is worth noting that the difference in lignin content between heat-treated and untreated wood reduces after weathering for 1512 h. All of the cell wall polymers such as cellulose, hemicelluloses, and lignin are hydroscopic. The order of hydroscopicity is: hemicellulose (HEMI)>cellulose>lignin (KLIG) [18]. Thus, the loss of lignin means an increase in the content of other components, and consequently surface can become more hydrophilic. The same observation is reported by Kalnins and Feist [19]. It is also reported that the wettability for Sitka spruce increased when exposed to xenon arc lamp radiation and water spray [20].

The OH/CH_2 ratios of untreated and heat-treated aspen before weathering and after weathering for 72 h and 1512 h are also shown in Figure 9. The OH/CH_2 ratio continuously increases for heat-treated aspen. For untreated aspen however, the ratio increases initially up to 72 h exposure time, and then remains the same. If the OH functional groups are responsible

for the increase of wettability, the tendency of the functional ratio is expected to increase with increasing weathering time. Thus, the tendency of OH/CH_2 ratios shown in Figure 9 suggests that, the affinities of specimens studied during the present work for water are attributable to the OH groups.

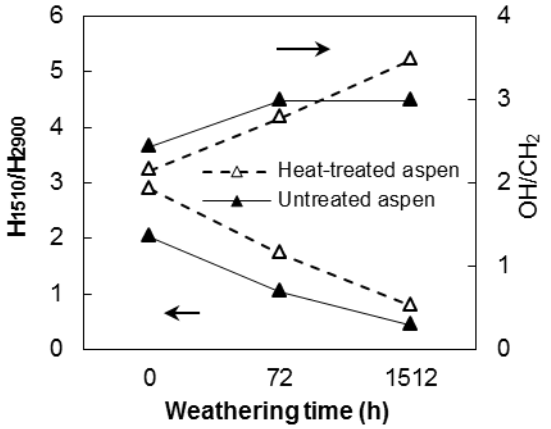

Figure 9 Evolution of the lignin loss and OH group change as a function of weathering time

CONCLUSIONS

Artificial weathering causes rapid aging of materials and gives an idea of how a material will behave under natural conditions over a relatively long time. In this work, the effect of artificial weathering on the modifications in wood surface properties for heat-treated aspen was studied using different methods.

The natural aging times corresponding to the exposure times used in artificial weathering tests in this study were estimated by comparing the total exposure of a sample to irradiation in the two cases (in the artificial aging chamber vs. in a natural environment such as Florida, USA).

The color behavior of heat-treated aspen under artificial weathering conditions was studied using spectrocolorimetry. The color changes differently on tangential and radial surfaces of aspen during aging. It was found that the color of the tangential surfaces was affected more than that of the radial surfaces.

The wettability of heat-treated aspen increased due to aging. XPS and FTIR results indicated that lignin decreases and OH group increases with aging, which contribute to the better wettability of heat-treated wood after weathering compared to an unweathered sample.

REFERENCES

[1] X. Huang, D. Kocaefe, Y. Boluk, Y. Kocaefe, A. Pichette, Effect of surface preparation on the wettability of heat-treated jack pine wood surface by different liquids, Eur. J. Wood Wood Prod., 70 (2012) 711-717.

[2] X. Huang, D. Kocaefe, Y. Kocaefe, Y. Boluk, C. Krause, Structural analysis of heat-treated birch (Betule papyrifera) surface during artificial weathering, Appl Surf Sci, 264 (2013) 117-127.

[3] X. Huang, D. Kocaefe, Y. Kocaefe, Y. Boluk, A. Pichette, Changes in wettability of heat-treated wood due to artificial weathering, Wood Sci Technol, 46 (2012) 1215-1237.

[4] X. Huang, D. Kocaefe, Y. Kocaefe, Y. Boluk, A. Pichette, Study of the degradation behavior of heat-treated jack pine (Pinus banksiana) under artificial sunlight irradiation, Polym Degradation Stab, 97 (2012) 1197-1214.

[5] X. Huang, D. Kocaefe, Y. Kocaefe, Y. Boluk, A. Pichette, A spectrocolorimetric and chemical study on color modification of heat-treated wood during artificial weathering, Appl Surf Sci, 258 (2012) 5360-5369.

[6] D. Kocaefe, X. Huang, Y. Kocaefe, Y. Boluk, Quantitative characterization of chemical degradation of heat-treated wood surfaces during artificial weathering using XPS, Surf Interface Anal, 45 (2013) 639-649.

[7] http://www.q-lab.com/products/q-sun-xenon-arc-test-chambers/q-sun-xe-1, in.

[8] R.W.G. Hunt, The Reproduction of Color, (1995).

[9] F.P.e.a. Incropera, Radiation:Processes and Properties, in: F.P. Incropera (Ed.) Fundamentals of Heat and Mass Transfer, John Wiley&Sons, New york, 2007.

[10] http://www.atlas-mts.com/, in.

[11] CABOT, UV weathering and related test methods, in: CABOT creating what matters.

[12] Q. Shen, P. Mikkola, J.B. Rosenholm, Quantitative characterization of the subsurface acid-base properties of wood by XPS and Fowkes theory, Colloids and Surfaces A: Physicochemical and Engineering Aspects, 145 (1998) 235-241.

[13] D.P. Kamdem, B. Riedl, A. Adnot, S. Kaliaguine, ESCA spectroscopy of poly (methyl methacrylate) grafted onto wood fibers, Journal of Applied Polymer Science, 43 (1991) 1901-1912.

[14] A. Koubaa, B. Riedl, Z. Koran, Surface analysis of press dried-CTMP paper samples by electron spectroscopy for chemical analysis, Journal of Applied Polymer Science, 61 (1996) 545-552.

[15] G. Sinn, A. Reiterer, S.E. Stanzl-Tschegg, Surface analysis of different wood species using X-ray photoelectron spectroscopy (XPS), Journal of Materials Science, 36 (2001) 4673-4680.

[16] G. Nguila Inari, M. Petrissans, J. Lambert, J.J. Ehrhardt, P. Gérardin, XPS characterization of wood chemical composition after heat-treatment, Surf Interface Anal, 38 (2006) 1336-1342.

[17] X. Colom, F. Carrillo, F. Nogués, P. Garriga, Structural analysis of photodegraded wood by means of FTIR spectroscopy, Polymer Degradation and Stability, 80 (2003) 543-549.

[18] C. Skaar, Wood-water relationships, Chemistry of Solid Wood. Adv. Chem., 207 (1984) 127-172.

[19] M.A. Kalnins, W.C. Feist, Increase in wettability of wood with weathering, Forest Prod J, 43 (1993) 55-57.

[20] H.-Y. Kang, S.-J. Park, Y.-S. Kim, Moisture sorption and ultrasonic velocity of artificially weathered spruce, Mokchae Konghak, 30 (2002) 18-24.